Journal of Catalysis **204,** 77–88 (2001)
doi:10.1006/jcat.2001.3361, available online at http://www.idealibrary.com on IDEAL®

# Heats of Adsorption of Linear NO Species on a $Pt/Al_2O_3$ Catalyst Using *in Situ* Infrared Spectroscopy under Adsorption Equilibrium

Abdennour Bourane,* Olivier Dulaurent,* Sophie Salasc,† Christian Sarda,†
Christophe Bouly,† and Daniel Bianchi*,[1]

*Laboratoire d'Application de la Chimie à l'Environnement (LACE), UMR 5634, Université Claude Bernard, Lyon-I, Bat. 303, 43 Bd du 11 Novembre 1918, 69622 Villeurbanne, France; and †FAURECIA Industries, BP 17, Bois sur prés, 25 550, Bavans, France

Received February 28, 2001; revised July 20, 2001; accepted July 24, 2001

**The adsorption of 1% NO/He on a reduced 2.9% $Pt/Al_2O_3$ catalyst is studied at several adsorption temperatures $T_a$ in the range 300–680 K using *in situ* FTIR spectroscopy. At 300 K several adsorbed NO species are formed on the Pt particles and on the support leading to numerous IR bands in the range 1850–1200 $cm^{-1}$. After a short duration of the adsorption, two main IR bands are detected at 1764 and 1710 $cm^{-1}$ assigned to two linear NO species (denoted by L) on defect and terrace sites of the Pt particles, respectively. The IR band at 1710 $cm^{-1}$ is not modified with the duration of the adsorption at 300 K while that at 1764 $cm^{-1}$ progressively decreases. Several IR bands are detected in the range 1650–1200 $cm^{-1}$ mainly due to the formation of nitrite and nitrate-adsorbed species on the support. The increase in $T_a$ from 300 to 540 K leads to a strong decrease in the IR band at 1710 $cm^{-1}$ while that at 1764 $cm^{-1}$ increases and shifts to 1778 $cm^{-1}$. For higher adsorption temperatures ($T_a < 680$ K), the IR band at 1778 $cm^{-1}$ progressively decreases with the increase in $T_a$. Cooling of the catalyst in 1% NO/He from 640 K leads to an increase in the IR band at 1778 $cm^{-1}$ and for the same value of $T_a$, the IR band intensities are similar during the heating and cooling stages. Similar to the analytical method previously developed for the determination of the heats of adsorption of linear and bridged CO species on several supported metal catalysts, the change in the intensity of the IR band of the L species adsorbed on defect sites with $T_a$ permits determination of the evolution of the coverage $\theta_L$ of this adsorbed species with $T_a$ at the constant NO pressure $P_a = 10^3$ Pa. It is shown that the curve $\theta_L = f(T_a)$ is in agreement with an adsorption model which considers: (a) an immobile adsorbed species and (b) a linear decrease in the heat of adsorption with the increase in $\theta_L$ in the range 0–1. This allows us to determine that the heat of adsorption of the L species on defect sites linearly varies with its coverage from $E_0 = 135$ kJ/mol at $\theta_L = 0$ to $E_1 = 105$ kJ/mol at $\theta_L = 1$. These values are in reasonable agreement with the literature data on Pt single crystals and polycrystalline Pt solids (foil and filament). It seems that it is the first time that the heats of adsorption of adsorbed NO species on supported Pt catalysts are determined probably because the present procedure is affected neither by the adsorption of other NO species nor by the NO dissociation; both processes create difficulties when using other classical analytical methods (temperature-programmed desorption and calorimetry).** © 2001 Academic Press

*Key Words:* **nitric oxide; chemisorption; platinum; FTIR; heat of adsorption; adsorption model.**

## 1. INTRODUCTION

The heats of adsorption of the adsorbed species (denoted by $E$) and their evolutions with the coverage $\theta$ of the sites (denoted by $E_\theta$ with $0 \leq \theta \leq 1$) constitute a fundamental parameter for characterization of the adsorption of the gases on supported metal catalysts because the values of $E_\theta$ quantify the coverage of the sites (according to classical definitions (1, 2)) under adsorption equilibrium. However, this parameter is rarely studied on supported metal catalysts because several experimental difficulties are linked to analytical methods such as temperature-programmed desorption (TPD) (3, 4), microcalorimetry (5, 6), and isosteric methods (7). In previous studies we have shown that, for the adsorption of CO on supported metal catalysts, the evolution of the IR band area (denoted by $A$) of the adsorbed CO species (i.e., linear and/or bridged CO species denoted by L and B, respectively) with the adsorption temperature $T_a$ for a constant adsorption pressure $P_a$ may allow us to determine the heats of adsorption of each adsorbed species and their evolutions with the coverage $\theta$ of the sites. The procedure is composed of two main steps: (a) the determination of the curve $\theta = f(T_a)$ at a constant adsorption pressure $P_a$ from the evolution of $A$ with $T_a$ and (b) the comparison of this experimental curve to that obtained from an adsorption model to determine $E_\theta$. This procedure has been applied for the determination of the heats of adsorption of L and/or B CO species formed on various supported (on alumina) metal catalysts: Pt (8–10), Pd (11), Rh (12), Ru (13), Cu (14), Pt/Rh (8), and Pd/Rh (12). Moreover, other metal oxide supports (i.e., $CeO_2/Al_2O_3$, $ZrO_2$) have also been studied (8, 15, 16).

In the present study the same procedure is applied to determine the heat of adsorption of a linear NO species

[1] To whom correspondence should be addressed. E-mail: daniel.bianchi@univ-lyon1.fr.



0021-9517/01 $35.00

adsorbed on a reduced $Pt/Al_2O_3$ catalyst. This allows us to show that the same adsorption model represents the evolution of the coverages of linear CO and NO species adsorbed on the Pt surface. Only the heat of adsorption values differ. It is also shown that this procedure is particularly well adapted to the objective of the present study because several adsorbed $NO_x$ species can be formed on the $Pt/Al_2O_3$ catalyst (in particular on the support), and NO can dissociate without affecting the measurement of the heat of adsorption of the L NO species. The determined $E_\theta$ values are compared to those in the literature on several Pt-containing solids (single crystals and polycrystalline Pt solids). The measurement of the heats of adsorption of NO species on a supported Pt catalyst is the preliminary step for the kinetic modeling of the catalytic reactions involving NO, such as NO dissociation, $NO/O_2$, and CO/NO.

## 2. EXPERIMENTAL

The 2.9%$Pt/Al_2O_3$ (in wt%, $\gamma$-$Al_2O_3$) catalyst was the same as that used and characterized in previous studies (8–10). For the FTIR study, the catalyst (or the support alone) was compressed to form a disk ($\Phi = 1.8$ cm, m = 40–200 mg), which was placed in the sample holder of a small internal volume stainless-steel IR cell (transmission mode) described elsewhere (8). This IR cell enabled *in situ* treatments (293–900 K) of the solid, at atmospheric pressure, with a gas flow rate in the range of 150–2000 $cm^3$/min. Before the adsorption of NO, the solid was treated *in situ* (150 $cm^3$/min) according to the following procedure: oxygen ($T = 713$ K, $t = 30$ min) $\rightarrow$ helium ($T = 713$ K, $t = 30$ min) $\rightarrow$ hydrogen ($T = 713$ K, $t = 1$ h) $\rightarrow$ helium ($T = 713$ K, $t = 10$ min) $\rightarrow$ helium (adsorption temperature). After this treatment, the dispersion of the metallic phase of the reduced catalyst using the adsorption of CO at 300 K and assuming a ratio CO/M = 1 was 85%, in agreement with literature data (6) on similar Pt catalysts. Similar dispersion values were obtained with hydrogen and oxygen chemisorption (H/M and O/M = 1) probably because the L CO species was the main adsorbed species. The same catalyst pellet was used for several experiments, and it was pretreated before each adsorption experiment as described previously. Note that the dispersion progressively decreased with the number of adsorption/pretreatment cycles (17): $\approx$50% after four cycles (stabilized dispersion). The heats of adsorption of NO were obtained on a stabilized solid according to the following procedure: after the pretreatment of the solid, a switch He $\rightarrow$ 1% NO/He (total pressure = 1 atm, flow rate in the range 200–600 $cm^3$/min) was performed at 300 K and then $T_a$ was slowly increased ($\approx$5–10 K/min) up to 700 K while the FTIR spectra of the adsorbed species were recorded periodically. Then the solid was cooled down to a temperature $T$ in the presence of 1% NO/He, and the FTIR spectrum was compared with that recorded at a similar temperature in the course of the heating stage. This comparison revealed the modifications of the surface in the course of the adsorption. The traces of $N_2O$ (13 ppm) and $NO_2$ (75 ppm) present in the 1% NO/He mixture were removed using a molecular sieve trap as described in (18). The amounts of NO, $N_2O$, and $NO_2$ at the outlet of the IR cell were analyzed using a second FTIR spectrometer with an IR gas cell (L = 20 cm, $V = 200$ $cm^3$). The dissociation of NO on $Pt/\gamma$–$Al_2O_3$ has been particularly studied by Lim *et al.* (19) in the 423–623 K range in comparison with Pt/C catalysts. Pt/C solids led to higher turnover numbers and selectivity in $N_2$ than the $Pt/Al_2O_3$ catalyst, which mainly yielded $N_2O$ (90% $N_2O$). In our present experimental conditions, the dissociation of NO on the $Pt/Al_2O_3$ solid was not followed with accuracy because the stainless-steel IR cell alone also led to a slight NO dissociation after a reduction treatment at 713 K. For instance, at 300 K using 200 $cm^3$/min of purified 1% NO/He mixture $\approx$50 ppm of $N_2O$ and $NO_2$ were recorded during a blank experiment with an empty IR cell. A treatment in 1% NO/He at $T > 573$ K suppressed the dissociation of NO at 300 K on the walls of the IR cell.

## 3. RESULTS

### 3.1. IR Spectra after Adsorption of NO at 300 K on $Pt/Al_2O_3$

Figure 1 gives the IR spectra recorded after the introduction of 1% NO/He (300 $cm^3$/min) at 300 K on the reduced $Pt/Al_2O_3$ solid. After 40 s, spectrum a shows that the NO adsorption leads to the appearance of several main IR bands at 1764, 1710, 1645, 1580, 1525, 1460, 1440, 1360, 1320, and 1230 $cm^{-1}$. Spectrum b indicates that some IR

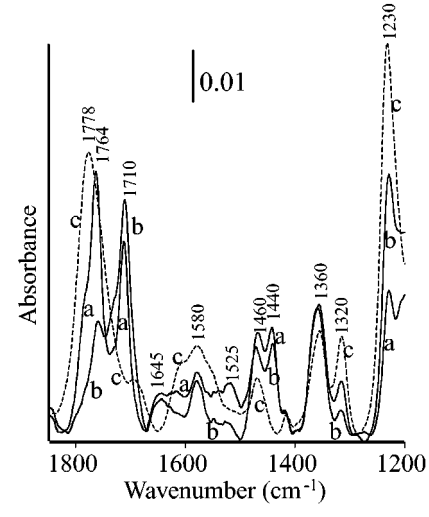


**FIG. 1.** FTIR spectra recorded on reduced stabilized 2.9% $Pt/Al_2O_3$ solid with the 1% NO/He mixture: (a) 40 s at 300 K; (b) 8 min at 300 K; and (c) at 500 K.

bands slightly increase with time on stream while that at 1764 $cm^{-1}$ decreases. The assignment of these IR bands to specific adsorbed $NO_x$ species on the surface is presented in the Discussion section. However, it is well known that L NO species on Pt-containing solids give IR bands in the range 1850–1650 $cm^{-1}$ on supported Pt catalysts (18–21) and on single crystals (22–24) while the IR bands of the B or bent NO species are situated at lower wavenumbers (20–24). Moreover, the studies on the adsorption of NO on supported Pt catalysts have shown that the IR bands below 1650 $cm^{-1}$ are mainly due to various $NO_x$ species adsorbed on the support (20, 25). Adsorption of 1% NO/He at 300 K on a disk of pure $Al_2O_3$ treated in $H_2$ at 713 K leads in the 1650–1200 $cm^{-1}$ range to IR bands very similar (same intensity) to those observed on $Pt/Al_2O_3$. At 300 K on $Al_2O_3$ the adsorption of 1% $NO_2$/He gives strong IR bands at 1625, 1593, 1564, 1293, and 1256 $cm^{-1}$ while there is no IR band after the adsorption of 1% $N_2O$/He. This indicates that the IR bands observed on $Pt/Al_2O_3$ below 1650 $cm^{-1}$ are due mainly to the adsorption of $NO_2$ and NO on the support. Considering that the present study is focused on the heats of adsorption of the L NO species on Pt sites, we only give in the following figures the IR bands observed in the range 1850–1650 $cm^{-1}$. Figure 2 shows the evolution of the IR bands with the duration of the adsorption at 300 K. After 20 s (Fig. 2a), it is observed that two IR bands at 1764 and 1710 $cm^{-1}$ (denoted B1 and B2, respectively) are associated with two shoulders at 1780 and 1730 $cm^{-1}$ (denoted S1 and S2, respectively), which strongly overlap B1 and B2. The increase in time on stream (Fig. 2) leads to a decrease in the intensities of B1 and S1 associated with the increase in S2. The intensity of B2 is not significantly affected by the duration of the adsorption at 300 K. Figure 3 compares the IR spectra recorded before (Fig. 3b) and after (Fig. 3c) a switch 1% NO/He → He performed after

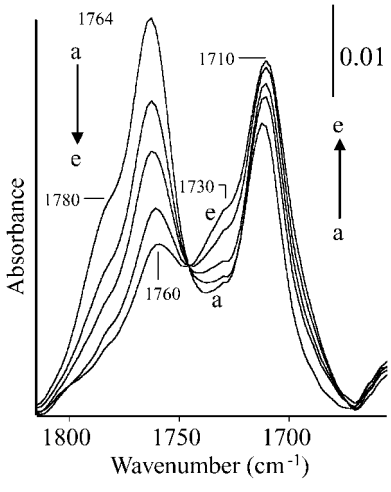


**FIG. 2.** Evolution of the IR bands of the L NO species with the duration of the adsorption at 300 K using the 1% NO/He mixture: (a–e) 20 s, 1 min, 2 min, 6 min, and 11 min.

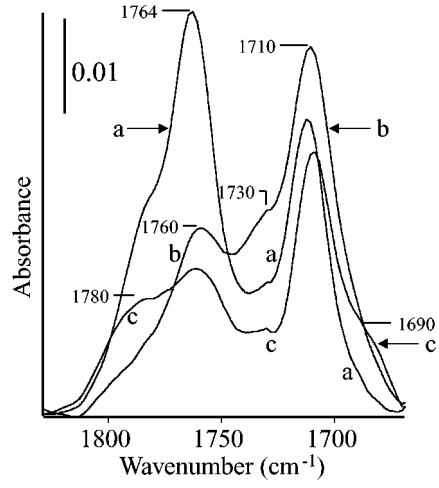


**FIG. 3.** Evolution of the IR bands of the L NO species with a helium treatment at 300 K: (a) 20 s in 1% NO/He; (b) 8 min in 1% NO/He; and (c) 40 s in helium after (b).

8 min of adsorption at 300 K. It can be observed that: (a) the intensities of B1 and B2 are not significantly affected by the desorption (strongly adsorbed NO species); (b) S2 disappears while S1 increases, thus indicating that in the presence of NO gas a weakly adsorbed species interacts with S2; and (c) a weak shoulder S3 is detected at 1690 $cm^{-1}$. Note that the intensity of B2 is similar in Fig. 3a (20 s of adsorption on a freshly reduced catalyst) and Fig. 3c (helium treatment), thus confirming that the adsorbed species characterized by B2 is not involved in the process leading to the decrease in B1. None of the IR bands below 1650 $cm^{-1}$ are affected by helium treatment. The introduction of 1% NO/He after 5 min of desorption provides an IR spectrum similar to that recorded before the helium treatment (Fig. 3b).

Considering that $Pt/Al_2O_3$ catalysts (19) and the walls of the IR cell may slightly dissociate NO, it can be considered that the modifications of the IR spectra in Fig. 2 are due to an accumulation on the surface of the products of the dissociation. However, the presence of NO gas is not necessary to observe the modifications of the IR bands as shown in Fig. 4. After 20 s of adsorption (Fig. 4a), a switch 1% NO/He → He is performed. It can be observed (Figs. 4b and 4c) that B2 is not modified while B1 decreases associated with the increase in S1 (which shifts to 1793 $cm^{-1}$) and with the appearance of the shoulder S3 at 1685 $cm^{-1}$. After 4.5 min in helium, S1 is detected as an IR band due to the strong decrease in the intensity of B1. After 5 min in helium a switch He → 1% NO/He leads after 20 s to spectrum d in Fig. 4, which indicates that B1 increases strongly without reaching its initial intensity (Fig. 4a). This difference between spectra a and d signifies that the decrease in B1 during the helium treatment is associated with a partial poisoning of the sites. However, this decrease is mainly due to the removal of the NO species from the Pt surface (the IR band increases after

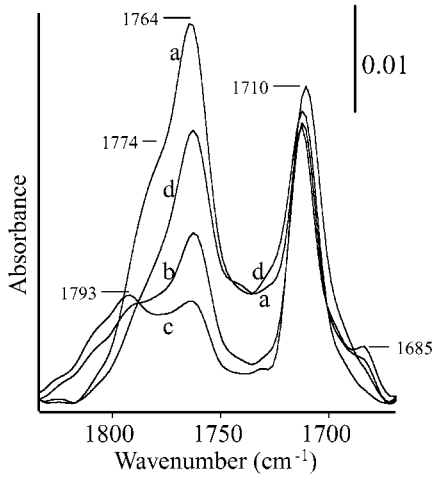


**FIG. 4.** Evolution of the IR bands of the L NO species with the duration of the helium treatment at 300 K: (a) 20 s in 1% NO/He; (b) 30 s in He; (c) 4.5 min in He; and (d) 20 s in 1% NO/He after (c).

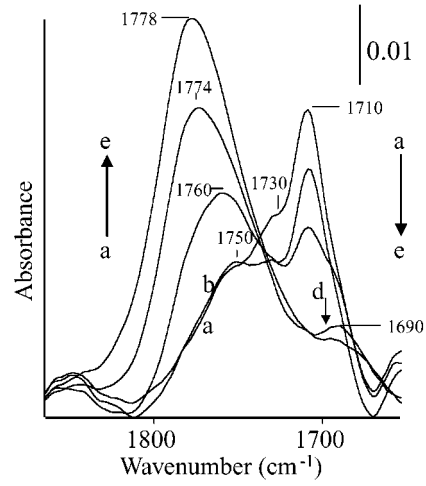


**FIG. 5.** Evolution of the IR bands of the L NO species with the increase in the adsorption temperature using the 1% NO/He mixture: (a–e) 320 K, 338 K, 378 K, 438 K, and 540 K.

the reintroduction of NO). We show herein that the heat of adsorption of this species at full coverage is too high to lead to a significant rate of desorption at 300 K. It seems more likely that the decrease in B1 is associated with the involvement of the adsorbed species ($NO_{ads}$) in the NO dissociation. It can be suggested that B1 decreases due to several processes: (a) the dissociation of $NO_{ads}$ ($NO_{ads} \rightarrow N_{ads} + O_{ads}$), (b) the production of $N_2O$ ($NO_{ads} + N_{ads} \rightarrow N_2O$), and (c) the interaction of the remaining $NO_{ads}$ with $O_{ads}$ or $N_{ads}$ leading to the increase in S1. The formation of $O_{ads}$ species may explain the poisoning of the sites forming the B1 species (compare Figs. 4a and 4d) because it has been shown that, on $Pt/Al_2O_3$ catalysts, there is an inhibition by oxygen due to a strong competition between $O_{ads}$ and $NO_{ads}$ species (19). This inhibition is not observed on Pt/C catalysts because the $O_{ads}$ species are removed by reaction with the support (19). The evolutions of S1 and S2 in Figs. 2–4 in correlation with that of B1 seem to indicate that they characterize the same adsorbed species: S1 is observed in helium while S2 is observed in the presence of NO gas. It can be considered that the shift from S1 to S2 in the presence of NO gas is due to a weakly adsorbed species which does not contribute significantly to the IR spectra shown in Figs. 2–4. Note that Amirnazmi *et al.* (26, 27) have postulated that the production of $N_2O$ in the NO dissociation on $Pt/Al_2O_3$ comes from a reaction between $NO_{ads}$ and $NO_g$ : $NO_g + NO_{ads} \rightarrow N_2O_g + O_{ads}$.

Some of these explanations of the modifications of the IR spectra during the NO adsorption at 300 K are speculative. However, this is not a crucial problem for the objectives of the present study, because it is shown that the increase in $T_a$, for the determination of the heat of adsorption of the L NO species, leads to a new and irreversible modification of the NO adsorbed/Pt system.

### *3.2. Evolution of the IR Bands of the Adsorbed $NO_x$ Species with $T_a$*

Figures 5 and 6 show the modifications of the IR spectra with the increase in $T_a$. In the range 300–540 K, it can be observed in Fig. 5 that B2 (1710 $cm^{-1}$) and S2 (1730 $cm^{-1}$) progressively decrease while B1 strongly increases and shifts to higher wavenumbers from 1750 $cm^{-1}$ at 300 K (after 20 min in 1% NO/He) to 1778 $cm^{-1}$ at 540 K. The IR bands below 1650 $cm^{-1}$ are slightly modified, except the IR band at 1440 $cm^{-1}$ which decreases and is no longer detected at 440 K (Fig. 1c). At 540 K, the disappearance of B2 permits clear detection of the shoulder at 1690 $cm^{-1}$. For $T_a > 540$ K, Fig. 6 shows that the intensity of B1 progressively decreases associated with a slight shift to higher

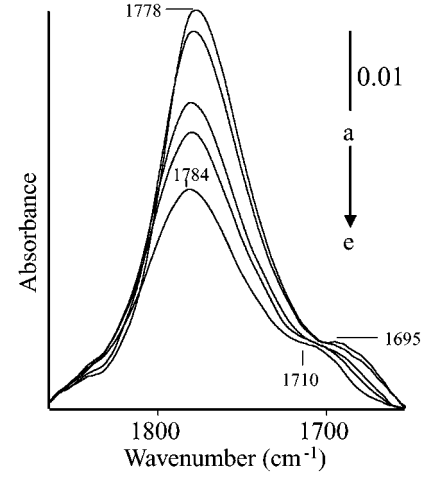


**FIG. 6.** Evolution of the IR bands of the L NO species with the increase in the adsorption temperature using the 1% NO/He mixture: (a–e) 540 K, 568 K, 598 K, 615 K, and 638 K.

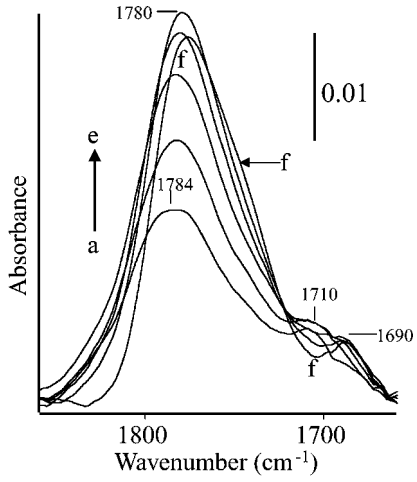


**FIG. 7.** Evolution of the IR bands of the L NO species with the decrease in the adsorption temperature using the 1% NO/He mixture: (a–f) 638 K, 598 K, 553 K, 523 K, 483 K, and 433 K.

wavenumbers (1784 $cm^{-1}$ at 640 K) without the appearance of a new IR band. The shoulder at 1690 $cm^{-1}$ shifts to 1710 $cm^{-1}$ associated with a slight decrease in intensity. The intensity of the B1 does not decrease with time on stream (<10 min) at 640 K indicating the absence of an accumulation of adsorbed species on the Pt surface (i.e., $O_{ads}$ species coming from the NO dissociation). The IR bands below 1650 $cm^{-1}$ decrease with the increase in $T_a$ but are still well detected at 640 K.

Figure 7 shows the evolution of the IR bands obtained upon cooling of the sample in 1% NO/He from 640 K to 430 K. The IR band at 1784 $cm^{-1}$ progressively increases with the decrease in $T_a$ in the range 640–540 K and is then constant from 540 to 480 K. For an adsorption temperature $T_a$ between 640 and 540 K, the same intensity is observed for the B1 IR band during the heating and the cooling stage. For temperatures lower than 450 K, this IR band slightly decreases and for temperatures lower than 370 K the evolution of the spectra is more complex (results not shown). The shoulder observed at 1710 $cm^{-1}$ at high temperatures progressively shifts to 1690 $cm^{-1}$ with the decrease in $T_a$.

In the Discussion section, the evolution of the intensity of B1, which is ascribed to a linear NO species, with $T_a$ is used for the determination of the heat of adsorption of this adsorbed species.

### *3.3. On the Modification of the Pt Surface during the NO Adsorption at High Temperatures*

The IR spectra in Figs. 5 and 6 clearly show that there is a modification of the Pt surface during the increase in $T_a$ between 300- and 540 K, leading to an increase in the intensity of B1 and to the decrease in B2. During the 1% CO/He adsorption on the same catalyst (8–10), a similar process has been observed in the same range of temperature for the intensity of the IR band of the L CO species which has been attributed to the reconstruction of the Pt surface. For the adsorption of NO, the reconstruction significantly affects the profile of the IR spectra in the 1850–1650 $cm^{-1}$ range. For instance, after cooling of the sample in 1% NO/He from 640 to 400 K, a switch 1% NO/He → He is performed and the temperature is raised to 740 K. After 10 min in helium at this temperature, the solid is cooled to 300 K and then 1% NO/He is introduced. Figure 8 compares the IR spectra recorded after this treatment (Fig. 8a) and on a freshly reduced solid (Fig. 8b) for a short duration of adsorption ($t_a$ = 20 s). It can be observed that the intensity of the IR band at 1764 $cm^{-1}$ (B1) is higher in Fig. 8a than in Fig. 8b while the opposite is observed for B2. The IR band at 1764 $cm^{-1}$ also decreases with time on stream in 1% NO/He on the reconstructed Pt surface, but with a lower rate than that on the freshly reduced solid. This is probably associated with a lower rate of NO dissociation.

The differences between Figs. 8a and 8b lead to the conclusion that the Pt surface reconstructs in the course of the adsorption of NO at high temperatures. There is a transformation of the Pt sites giving the B2 IR band into the sites giving the B1 IR band. On single crystals the reconstruction of the surface in the presence of NO is a well-known process (28–30), and Amirnazmi and Boudart (26) also have considered a slow rearrangement of reduced Pt surface on $Pt/Al_2O_3$ during the NO dissociation. Figure 8 shows that the modifications of the Pt surface by reconstruction are irreversible and NO is adsorbed differently after the two pretreatments of the catalyst: reduction in $H_2$ and adsorption of NO at high temperatures. This reconstruction of the surface only disappears after a new reduction procedure (same spectrum as Fig. 8b after adsorption of NO at 300 K).

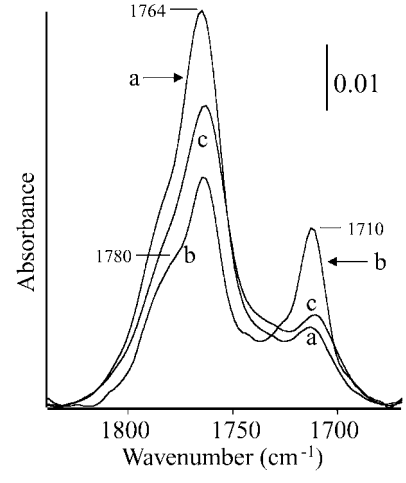


**FIG. 8.** Irreversible modification of the IR spectra with the NO adsorption at high temperatures: (a) at 300 K after 20 s in 1% NO/He on a solid treated in NO/He at 638 K and then in helium at 713 K; (b) 20 s in 1% NO/He on a freshly reduced solid; and (c) 3 min after (a).

## 4. DISCUSSION

The main objective of the present paper is the determination of the heat of adsorption of the adsorbed species leading to the B1 IR band. In the first step the IR bands observed in the range 1850–1200 $cm^{-1}$ are assigned to specific adsorbed species.

### *4.1. Assignment of the IR Bands in the Range 1850–1650 $cm^{-1}$*

It seems that there is an agreement in the literature to consider that the adsorption of NO on Pt-containing solids leads to L (linear) and B (bridged or bent) NO species. These species are identified by the position of their IR bands (IR, IRAS, EELS). Roughly L and B species give IR bands in the ranges 1850–1650 $cm^{-1}$ and 1650–1400 $cm^{-1}$, respectively (see Table 1 in Ref. (31)). For instance, on Pt(112) Heiz *et al.* (24) assign two IR bands at 1794 and 1698 $cm^{-1}$ to L species on steps and terraces, respectively, and two IR bands at 1601 and 1441 $cm^{-1}$ to B species on steps and terraces, respectively. Similar assignments have been proposed on Pt(111) (22, 23) and Pt(110) (30). These various studies show that an IR band in the range 1850–1650 $cm^{-1}$ is due to an L NO species. The position of the IR band depends on the nature of the Pt sites: IR bands around 1800 $cm^{-1}$ and 1700 $cm^{-1}$ are ascribed to defect and terrace sites, respectively (24). Agrawal and Trenary (32) have specifically considered the role of the defect concentration (on three vicinal Pt(111)) on the FTIR spectra of adsorbed NO species. Their study (32) reveals the complexity of the NO adsorbed species/Pt surface system which may change with $\theta$ and $T_a$, as well as with the defect concentration. However, they conclude that defect sites lead to two IR bands at 1810–1840 $cm^{-1}$ and 1600–1640 $cm^{-1}$ due to L and B NO species, respectively (32). The terrace sites lead to IR bands at 1716–1720 $cm^{-1}$ and 1480–1510 $cm^{-1}$ for L and B NO species, respectively (32). Levoguer and Nix (31) have confirmed using a polycrystalline Pt foil that defect sites give an IR band at $\approx$1800 $cm^{-1}$ for L species.

On the reduced $Pt/Al_2O_3$ catalyst, it is observed in Fig. 2 that a short duration of adsorption (1% NO/He) leads to two main IR bands B1 and B2 at 1764 and 1710 $cm^{-1}$, respectively, associated with two shoulders S1 and S2 at 1780 and 1730 $cm^{-1}$. Considering the results on single crystals and Pt foils (22–24, 30–32), it can be considered that B1 and B2 are L species on defect and terrace sites, respectively. In the literature, the adsorption of NO on supported Pt catalysts—2% $Pt/Al_2O_3$ (20), 5% $Pt/SiO_2$ (33), 2% $Pt/TiO_2$ (34), and 6% $Pt/SiO_2$ (35)—mainly leads to an IR band at $\approx$1765 $cm^{-1}$ associated with small shoulders at $\approx$1700 $cm^{-1}$. In these studies (20, 33–35), the IR band at $\approx$1765 $cm^{-1}$ is ascribed to a linear NO species while the shoulder at $\approx$1700 $cm^{-1}$ is ascribed either to nonlinear or bent species (20) or not assigned (33). The results observed in Fig. 2 differ from these studies on Pt-containing catalysts because we observe two IR bands of similar intensity at 1772 and 1710 $cm^{-1}$ after a short duration of adsorption while a main IR band was previously observed at $\approx$1770 $cm^{-1}$ with some shoulders around 1710 $cm^{-1}$ (20, 33–35). Note that this is the situation for the spectra in Figs. 8a and 8c obtained on a reconstructed Pt surface with a main IR band at 1764 $cm^{-1}$ and a small shoulder at 1710 $cm^{-1}$.

After adsorption of NO at 300 K on a reduced solid, there is a slow process either in the presence of 1% NO/He or in helium leading to a decrease in B1 associated with the increase in the shoulders. B2 is not significantly modified by this process (Figs. 3 and 4). In the presence of NO (Fig. 2), the decrease in B1 leads to the increase in S2 (1730 $cm^{-1}$) while in helium (Fig. 4) it leads to the increase in S1 (1793 $cm^{-1}$). This indicates a correlation between S1 and S2 which is confirmed by the fact that a treatment in helium after several minutes in 1% NO/He leads to the decrease in S2 and to the increase in S1 (Fig. 3). We have considered that the slow decrease of B1 is due to the involvement of the L species on defect sites in several processes (other than the desorption) linked to its dissociation. We suggest that S2 and S1 are due to L species on defect sites in interaction with $O_{ads}$ or $N_{ads}$ species. The effect of the presence of NO gas on the location of the shoulder is probably linked to the presence of a weakly adsorbed species. This species has not been detected with the present analytical procedure. However, (a) a weakly adsorbed NO species have been detected on Pt single crystals by a TPD peak at 200 K (22, 23), and (b) it has been reported (20) that the presence of NO gas affects the profile of the IR spectra in the range 1850–1650 $cm^{-1}$.

Figure 5 shows that raising $T_a$ leads to a reconstruction of the NO adsorbed species/Pt surface system: at high temperatures mainly B1 (L species on steps/defects) is recorded. This is in agreement with the studies performed on Pt-containing catalysts for a high adsorption temperature. For instance, on $Pt/SiO_2$ (18) the adsorption of NO at 493 K provides a main IR band at 1795 $cm^{-1}$ (L species) with a shoulder at 1620 $cm^{-1}$ (B species), while on $Pt/CeO_2$–$Al_2O_3$ (21) a single IR band is reported at 1755 $cm^{-1}$ for NO adsorption at 573 K. Note that the results in Figs. 5 and 6 cannot be interpreted considering that the coverage of the L species on terrace sites (B2 IR band) decreases with the increase in $T_a$ (low heat of adsorption for this species), because this IR band is not detected with the same intensity after cooling of the sample in NO/He. The decrease in the intensity of B2 is associated with the increase in B1 due to the modification of the adsorption sites. This is observed in Fig. 8 comparing at 300 K the intensities of the IR bands on a freshly reduced solid (Fig. 8b) and on a solid treated in NO/He at high temperatures (Fig. 8a). These results indicate that there is a reconstruction of the Pt surface with the increase

in $T_a$, leading to a transformation of the terrace sites (B2 IR band) into defect sites (B1 IR band). On the single crystal the reconstruction of the Pt surface in the presence of adsorbed NO is considered in several studies (28–30). Another possible interpretation of the modification of the IR spectra with the increase in $T_a$ is to consider that the O and/or N adsorbed species accumulated on the Pt surface at low temperatures are eliminated by reaction with NO.

### 4.2. Assignment of the IR Bands Below 1650 $cm^{-1}$

Intensities below 1650 $cm^{-1}$ (Fig. 1) are weak, indicating a low concentration of the adsorbed species on the surface. For instance, the adsorption of 0.1% $NO_2$/He at 300 K on $Al_2O_3$ leads to IR band intensity higher by a factor of 20, compared to the highest IR band observed on $Pt/Al_2O_3$ after adsorption of NO. The assignment of the IR bands observed below 1650 $cm^{-1}$ is speculative due to the complexity of the spectra. However, it seems that they are mainly due to the formation of nitrite and nitrate on the support (36–40). For instance the assignments can be (36, 39, 40): (a) 1230 and 1320 $cm^{-1}$ are the asymmetric and symmetric stretches of bridged nitrite, (b) 1460 and 1360 $cm^{-1}$ are the asymmetric and symmetric stretches of monodentate nitrite; and (c) the weak IR bands at 1645, 1580, and 1525 $cm^{-1}$ are the asymmetric stretches of small amounts of bridged, bidentate, and monodentate nitrate, respectively (symmetric stretch <1100 $cm^{-1}$). The IR band at 1440 $cm^{-1}$ in Fig. 1 which disappears during the increase in $T_a$ may correspond to linear nitrite (36, 40). However, it can also be due to B NO species adsorbed on the Pt terrace sites (24, 32). Indeed, this IR band behaves similarly to the B2 IR band decreasing and disappearing in the same range of adsorption temperature. Similarly the IR band at 1645 $cm^{-1}$ which disappears during the increase in $T_a$ (Fig. 1c) may be due to B species on steps (24, 32).

### 4.3. Heat of Adsorption of the Linear NO Species

From the study of the evolution of the IR bands in the range 1850–1650 $cm^{-1}$ with the increase in $T_a$, it must be considered that there is a reconstruction of the NO adsorbed/Pt surface system leading to a situation where the IR band of the L NO species on defect sites dominates the IR spectra. After treatment in 1% NO/He at $T_a > 500$ K the catalyst can be considered as stabilized: the intensities of B1 are similar during the heating and cooling stages (Figs. 5, 6, and 8). This allows us to determine the heat of adsorption of this adsorbed species (L species on steps) using the change in its IR band area with $T_a$.

Curve a in Fig. 9 provides at $T_a \geq 400$ K the change in the coverage $\theta_L$ of the L NO species on defect sites with $T_a$ at a constant adsorption pressure $P_a = 1000$ Pa using the data in Figs. 5 and 6. The coverage is obtained using the ratio between the IR band area at $T_a$ and the highest IR band

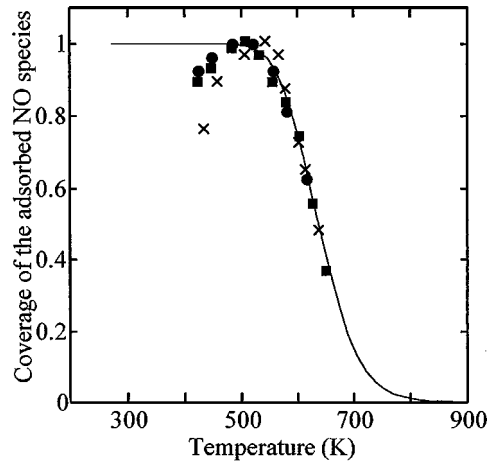


**FIG. 9.** Evolution of the coverage of the L NO species on defect sites according to the adsorption temperature: ×, experimental data with $P_a = 10^3$ Pa during the heating step; ●, experimental data with $P_a = 10^3$ Pa during the cooling step; ■, experimental data with $P_a = 10^3$ Pa for another experiment at higher temperatures;—, theoretical curve according to the adsorption model (see the text).

area (at $T_a \approx 540$ K) and considering that: (a) the intensity of the IR band is proportional to the amount of the L NO species on the surface; and (b) the IR absorption extinction coefficient is independent of $T_a$. We previously showed (17) that these assumptions were valid for the L CO species on the present $Pt/Al_2O_3$ catalyst. Figure 9a shows that $\theta_L$ (a) increases from 400 to 550 K (reconstruction and increase in the number of sites), (b) is constant between 550 and 580 K, and (c) linearly decreases for $T_a > 580$ K. Curve b in Fig. 9 corresponds to the $\theta_L$ values determined during the cooling stage after adsorption at 640 K. It can be observed that curves a and b are superimposed in the range 640–550 K, while for lower temperatures the coverage in curve b is constant in the range 550–480 K and slightly decreases for $T_a < 480$ K. We discuss the absence of poisoning of the sites during the adsorption at high temperature in relation to the NO dissociation. For $T_a < 480$ K the intensity of B1 decreases slightly by 10% probably due to a decrease in the number of sites (we have not investigated this process). Curve c in Fig. 9 corresponds to another experiment where $T_a$ was increased up to 680 K. The experiments leading to curves a–c in Fig. 9 have been repeated without observing significant differences, proving the repeatability of the data.

The curve $\theta_L = f(T_a)$ at $P_a = 1000$ Pa permits the determination of the heats of adsorption of L NO species using the adsorption model previously described for the determination of the heats of adsorption of L and B CO species on several supported metal catalysts (8–16 and references therein). This model assumes that (a) the adsorbed species are immobile and (b) the heats of adsorption linearly decrease with increase in coverage. Assumption (a) permits consideration that the adsorption coefficient K (ratio of the

rate constants of adsorption and desorption) is given by statistical thermodymanics (41, 42),

$$K = \frac{h^3}{k \times (2 \times \pi \times m \times k)^{3/2}} \times \frac{1}{T_a^{5/2}} \times \exp\left(\frac{Ed - Ea}{R \times T_a}\right), \quad [1]$$

where $h$ is Planck's constant; $k$ is Bolztmann's constant; $m$ is the mass of the molecule ($30 \times 10^{-3}$ kg/$6.02 \times 10^{23}$); $T_a$ is the adsorption temperature; $Ed$ and $Ea$ are the activation energies of desorption and adsorption, respectively; and $Ed - Ea$ is the heat of adsorption (denoted by $E$). Assumption (b) leads to an expression of the coverage for an adsorbed species given by (Refs. (8–16) and references therein)

$$\theta = \frac{R \cdot T_a}{\Delta E} \ln\left[\frac{1 + K_0 P_a}{1 + K_1 P_a}\right], \quad [2]$$

where $\Delta E$ is the difference in the heats of adsorption at $\theta = 0 (E_0)$ and $\theta = 1 (E_1)$; $K_0$ and $K_1$ are the adsorption coefficients at $\theta = 0$ and $\theta = 1$, respectively; and $T_a$ and $P_a$ are the adsorption temperature and pressure, respectively. For the determination of $E_1$ and $E_0$ we only have to find the values to be used in [1] and [2] to obtain the best fit between experimental and theoretical coverage values. For instance, curve d in Fig. 9 is obtained using $E_0 = 135$ kJ/mol and $E_1 = 105$ kJ/mol in expressions [1] and [2]. A very good agreement between the theoretical coverage (curve d) and the experimental data (curves a–c) is observed. This shows that the same adsorption model is valid to represent the adsorption of CO (L and B species (8–10)) and NO (L species) on the present $Pt/Al_2O_3$ catalyst. Note that the above heats of adsorption correspond to the activation energies of desorption considering that the NO adsorption is not activated. Assuming first order for the desorption of the L NO species, the evolution of its coverage $\theta$ with time of desorption $t$ is given by

$$\frac{-d\theta}{dt} = \frac{kT}{h} \exp\left(-\frac{E_d(\theta)}{RT}\right)\theta, \quad [3]$$

with $E_d(\theta)$ varying according to a linear relationship from 105 kJ/mol at $\theta = 1$ to 135 kJ/mol at $\theta = 0$. Simple calculations similar to those previously described (11, 14) show that the coverage of the L NO species cannot significantly decrease at 300 K. This confirms that the decrease in B1 during the helium treatment at 300 K (Fig. 3) does not involve a desorption process but more likely the NO dissociation.

The evolution of the coverage of the L NO species with $T_a$ is in very good agreement with an adsorption model, while it is known (19) that Pt may dissociate NO for $T > 400$ K. This indicates that the NO dissociation has no effect on the coverage of the L NO species. A simple explanation is to consider that the L NO species on step/defect sites is not an intermediate in the NO dissociation and that another adsorbed species is the active species (i.e., L NO species on terrace sites). However, we have previously shown for several reactions involving CO—$CO/O_2$ (43), $CO/H_2$ (44), and $CO/H_2O$ (45)—that for some CO/second reagent ratios, the rate of the surface elementary step implying the linear CO species does not lead to a significant modification of the adsorption equilibrium. For instance, in the range 400–740 K, the coverage of the L species for a 1% CO/0.25% $O_2$/He mixture is similar to that recorded with 1% CO/He. (This is not true for $CO/O_2$ ratios <2.) However, the $CO_2$ production is detected in the presence of $O_2$, and we have proved (43) that the linear CO species is an adsorbed intermediate species in the $CO_2$ production. For the present catalyst, it can be considered that the dissociation of NO via the L NO species on defect sites has no significant influence on the adsorption equilibrium (see Section 4.5).

### *4.4. Comparison of the Present Heat of Adsorption with the Literature Data*

The determination of the heat of adsorption of adsorbed NO species on Pt containing solids is mainly performed using a TPD procedure. On various Pt single crystals and polycrystalline Pt (foils or filaments), the TPD spectra (23, 30, 31, 46–55) reveal two peaks. The high temperature peak (denoted $T_H$), situated in the range 400–500 K, is the single peak observed at low coverage of the surface. The low temperature TPD peak (denoted $T_L$), situated in the range 300–400 K, appears and increases at high coverage. At saturation coverage, $T_H$ may appear as a shoulder of $T_L$. If the adsorption of NO is performed at low temperature (80 K), a third peak is observed in the 100–200 K range, due to a weakly adsorbed NO species (22, 23). There is a production of $N_2$ associated with $T_H$ due to the NO dissociation. The amount of NO dissociated depends of the single crystal. At saturation coverage the dissociation fractions are between 66 and 98% on Pt(100), Pt(411), Pt(211) (52), and Pt(410) (51), while values <15% are observed on Pt(111) and Pt (110) (49, 51). NO dissociation is also observed on polycrystalline Pt foils (53), and the dissociation fraction is a function of the coverage: 100% at low coverages (<0.12 L). This has also been observed on stepped Pt single crystals: the dissociation fraction was 100% below $\theta = 0.1$ and 30% at saturation (47). Table 1 gives the activation energy of desorption (denoted by $E_d$) associated with the $T_H$ and $T_L$ peaks on various Pt-containing solids. We have not collected any data on supported Pt catalysts. This is probably linked to the fact that there is a strong dissociation of NO during the TPD experiment as observed on model $Pt/CeO_2$ (56) and $Pt/Al_2O_3$ (57) catalysts.

The difficulty in the comparison with the values determined in the present study and those in Table 1 is the identification of the TPD peak to specific NO species. Gland and Sexton (22) on Pt(111) and Gorte and Gland (30) on Pt(110) have shown that there is not a simple correlation

**TABLE 1**

**Activation Energies of Desorption of NO for the Low ($T_L$) and High ($T_H$) Temperature TPD Peaks on Various Pt-Containing Solids**

| | $T_L$ peak | | | $T_H$ peak | | | |
|---|---|---|---|---|---|---|---|
| Single crystal | $E_d$ (kJ/mol) | $\nu$ ($s^{-1}$) | $\theta$ | $E_d$ (kJ/mol) | $\nu$ ($s^{-1}$) | $\theta$ | References |
| Pt(111) | 104 | $10^{16}$ | >0.3 | 140 | $2 \times 10^{18}$ | n.i | 49 |
| Pt(110) | (∗) | (∗) | (∗) | 140 | $10^{16}$ | n.i | 30, 49 |
| Pt(100) | 92 | $10^{16}$ | n.i | 140 | $10^{16}$ | n.i | 49 |
| Pt(110) | 96 | $10^{13}$ | n.i | 116 | $10^{13}$ | n.i | 46 |
| Pt(111) | n.o | n.o | | 115 | $10^{13}$ | n.i | 46 |
| Pt(S)-[12(111) × (111)] | 85.8 | $10^{13}$ | n.i | 108.4 | $10^{13}$ | n.i | 47 |
| Pt(211) | 123 | $3 \times 10^{17}$ | n.i | 275–204[a] | $10^{29}$[a] | 0–1 | 52 |
| Pt foil | 113–92 | $10^{16}$ | 0 to 1 | 159–146 | $10^{16}$ | 0–1 | 53 |
| Pt filament | 113–99 | $10^{16}$ | 0 to 1 | 148–132 | $10^{16}$ | 0–1 | 55 |

*Notes.* n.i., not indicated; n.o., not observed; (∗), weak TPD peak.
[a] Apparent activation energy and preexponential factor.

between the TPD peaks and the adsorbed NO species detected by their vibrational frequencies. At low coverages there is only the IR band of the B species while only the $T_H$ peak is detected which indicates that the B species contribute to this TPD peak. However, the increase in the coverage leads to the removal of the IR band of the B species and to the appearance of those of the L species (22, 24, 30, 49), while two peaks are detected on the TPD spectra. For the adsorption of CO on Pt-containing solids there is similar difficulty in correlating IR and TPD spectra. However, there is an agreement in the literature (see references in Ref. (17)) that the high and low TPD peaks are associated with step and terrace sites, respectively. Xu *et al.* (58, 59) have determined the following order of stability for the adsorbed CO species: L on steps >B on steps >L on terraces >B on terraces. For the adsorption of NO on Pt(112) Heiz *et al.* (24) have shown using IRAS that the four similar NO species can be simultaneously present on the surface. The involvement of step and/or defect sites on the $T_H$ peak of the NO TPD spectra is considered by several authors (50, 52–54). This shows that the heat of adsorption of the L NO species on step/defect sites characterized by the B1 IR band must be compared to $E_d$ obtained from the $T_H$ TPD peak. Table 1 shows that $E_0 = 135$ kJ/mol found in the present study is in reasonable agreement with several values on single crystals and polycrystalline Pt solids, even if the coverages are indicated rarely in the literature. The $E_d$ values obtained from the $T_H$ peak are not strongly dependent of the exposed face as commented by Lee *et al.* (60). The authors note that one key unexplained observation is that experimental heats of adsorption of simple molecules (i.e., CO, NO) on Pt vary only modestly with changing surface structure (steeped or kinked surface, closely packed planes). They suggest that reconstruction and relaxation on the electronic coordination numbers of the surface atoms lead to surface atoms having about the same electronic coordination numbers as Pt(111) surface atoms, whatever the initial surface. This may explain that we determine a value in reasonable agreement with the literature on single crystals. Note that two studies (53, 55) indicate a decrease in $E_d$ with the increase in the coverage as observed in the present studies. However, at high coverages, the values in Refs. (53, 55) differ from $E_1 = 105$ kJ/mol.

A better agreement is observed with the studies which determine $E_d$ using molecular beam scattering (48, 54). For the $T_H$ peak, Lin and Somorjai (48) have determined 120 kJ/mol on Pt(111) and 135 kJ/mol on Pt(557). For the $T_H$ peak on Pt(111), Campbell *et al.* (54) have determined 138 kJ/mol at $\theta \approx 0$ in good agreement with $E_0 = 135$ kJ/mol. The increase in $\theta$ from 0 to 0.05 leads to a linear decrease in $E_d$ (54). At $\theta = 0.05$, a drop is observed to 113 kJ/mol (formation of the adsorbed species giving the $T_L$ peak). Then the increase in $\theta$ is associated with the linear decrease in $E_d$ to 75 kJ/mol at $\theta = 0.25$ assigned to repulsive interactions (54). This linear decrease in $E_d$ agrees with that determined in the present study, even if the values at full coverage differ because the comparison does not involve the same species ($T_H$ peak in the present study, $T_L$ peak in Ref. (54)).

The heat of adsorption of the L NO species on defect sites determined in the present study can be compared to the values obtained by Yeo *et al.* (61) on Pt(100) using single crystal adsorption calorimetry. The authors study three different initial states of the surface: (1 × 1), hex, and hex sputtered (hex sp). They observe that the heats of adsorption at low coverage significantly differ with the nature of the surface: 200 kJ/mol on (1 × 1) and 175 kJ/mol on hex and hex sp. On hex and hex sp, the heat of adsorption almost linearly decreases to 105 kJ/mol at $\theta = 1$, while on (1 × 1) the heat of adsorption also decreases to 105 kJ/mol, but with a more complex profile due to the reconstruction of the hex surface to (1 × 1) surface. Note the good agreement between the values of Yeo *et al.* (61) at full coverage of the surfaces (105 kJ/mol) and $E_1 = 105$ kJ/mol determined with our procedure on $Pt/Al_2O_3$. At low coverage $E_0 = 135$ kJ/mol

differs from 200 kJ/mol on (1 × 1) and 175 kJ/mol on the hex surface (61). Yeo *et al.* (61) have also studied the adsorption of CO on the same Pt surface, and a good agreement was observed with the results obtained by our procedure for the L CO species on the present $Pt/Al_2O_3$ solid (9, 10). This remark may explain the difference at low coverage in the two studies. Probably Yeo *et al.* (61) characterize the heat of adsorption of the B NO species on steps formed at low exposure (24, 29, 31, 32, 62), while our procedure only involves the L NO species. The good agreement previously observed between the two analytical procedures for the measurement of the heat of adsorption of CO (9, 17) is because the same species (L CO species on steps) was characterized in the two studies (10, 58, 59). The agreement observed with Ref. (61) at high coverage (105 kJ/mol) is because at saturation coverage, the L species dominates the NO adsorption.

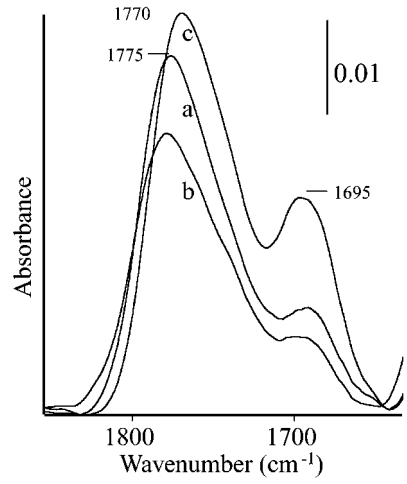


**FIG. 10.** Modifications of the IR spectra of the L NO species after several treatments at 453 K: (a) after cooling from 638 K in 1% NO/He; (b) in 1% NO/He after a treatment for 3 min in $O_2$; and (c) in 1% NO/He after treatment for 3 min in $H_2$ following (b).

### *4.5. Heat of Adsorption of NO and NO Dissociation*

The overlap of curves a and b in Fig. 9 clearly indicates that there is no decrease in the number of Pt sites adsorbing the L NO species. At first view, this may seem surprising if one considers that the NO dissociation may produce strongly adsorbed $O_{ads}$ species. Moreover, the difference between $E_0$ and the values at low coverages in (61) may be due to the presence of oxygen species on the surface. Yeo *et al.* (61) indicate that their measurements are performed in the absence of significant NO dissociation while NO can be dissociated on $Pt/Al_2O_3$ for $T_a > 400$ K (19). Campbell *et al.* (54) have studied the effect of oxygen precovered surface ($\theta_O = 0.25$) on the $E_d$ values of NO species at low coverage. The authors observe that the preadsorption of $O_2$ has no marked influence on the amount of adsorbed NO but leads to a decrease in $E_d$ from 138 to 77 kJ/mol. However, the following experiments show that the impact of eventual $O_{ads}$ species coming from the NO dissociation (19) on the number and the coverage of the step/defect sites adsorbing the L NO species is very limited.

Spectrum a in Fig. 10 is recorded at 453 K after cooling from 640 K in the presence of 1% NO/He. After a switch 1% NO/He → He leading to the disappearance of the IR band of the L NO species, pure $O_2$ is introduced for 3 min and then after a purge in helium for 3 min, a switch He → 1% NO/He is performed, leading to spectrum b in Fig. 10. Note that strongly adsorbed $O_{ads}$ species on Pt-containing solids only desorb at $T > 600$ K in TPD experiments (63) due to a very high heat of adsorption (64). It can be observed that the $O_2$ treatment has a limited influence on the intensity of the IR band of the L species on step/defect sites, indicating either that these sites do not strongly chemisorb oxygen or that NO rapidly displaces or reacts with the $O_{ads}$ species. This in agreement with the observations (a) of Campbell *et al.* (54) (oxygen does not modify the amount of adsorbed NO species) and (b) of Agrawal and Trenary (32) on Pt(111) who indicate that the IR band of the L species on steps (1831 $cm^{-1}$) was not strongly affected by preadsorbed oxygen. Considering that the heat of adsorption of $O_2$ on Pt is strongly higher (>200 kJ/mol (64)) than that of NO (<135 kJ/mol), the displacement of $O_{ads}$ by NO seems improbable. It is more likely that $O_{ads}$ species react with NO gas according to the elementary step $NO_g + O_{ads} \leftrightarrow NO_2$ which is involved in the $NO/O_2$ reaction on $Pt/Al_2O_3$ (63). This explains that curves a and b are superimposed in Fig. 9 because the $O_{ads}$ species formed during the NO dissociation are removed by reaction with $NO_g$. Moreover, Figs. 10a and 10b show that the coverage of the L NO species is not significantly decreased after the oxygen treatment, indicating that the heat of adsorption of the L species is not strongly modified. After the experiment leading to Fig. 10b, a switch 1% NO/He → He is performed and then pure hydrogen is introduced for 3 min. After a purge in helium, 1% NO/He is introduced, leading to spectrum c in Fig. 10. It can be observed that (a) the intensity of the IR band of the L species on defect sites is similar to that observed before the $O_2$ treatment associated with a slight shift to a lower wavenumber (1770 $cm^{-1}$) and (b) the intensity of the IR band at 1695 $cm^{-1}$ (L species on terrace sites) significantly increases. These results show that strongly adsorbed $O_{ads}$ species have no strong influence on the coverage of the L NO species on step/defect sites, but that they block the sites adsorbing the L species on terrace sites. Note that the fact that the IR band at 1695 $cm^{-1}$ is detected in Fig. 10c at 453 K indicates that the heat of adsorption of L species on terrace sites is probably of the order of magnitude of that of the L species on steps. Assuming that L species on terraces contribute to the $T_L$ peak in Table 1, the above remark is in agreement with the limited difference between the $E_d$ values obtained from the two TPD peaks. However,

the terrace sites strongly adsorb oxygen (compare Figs. 10b and 10c), and this explains that during the NO adsorption (Figs. 5 and 6), the B2 IR band is not detected at high temperatures due to (a) the surface reconstruction and (b) the adsorption of oxygen species coming from the NO dissociation. After Fig. 10c, the IR band at 1695 $cm^{-1}$ decreases progressively with time on stream in 1% NO/He. Data in Fig. 10 clearly show that on the Pt surface some sites can be strongly affected by adsorption of $O_2$ while other sites are not affected, in particular those giving the IR band used in the present study to determine the heat of adsorption of L NO species. This heterogeneity in the Pt sites to oxygen poisoning also is observed on supported Pt catalysts (18) and on a Pt foil (31). Finally, it must be considered that with our procedure the NO dissociation has a limited influence on the measurement of the heat of adsorption of the L NO species on the Pt step/defect sites.

From the above discussion, it can be considered that the values of the heat of adsorption of the L NO species on defect sites found in the present study linearly decreasing with the increase in $\theta_L$ from $E_0 = 135$ kJ/mol at $\theta_L = 0$ to $E_1 = 105$ kJ/mol at $\theta_L = 1$ are in reasonable agreement with the data on single crystals and polycrystalline Pt solids, and this supports the views of Lee *et al.* (60). To our knowledge it is the first time that the heat of adsorption of NO on supported Pt catalysts is determined. For instance, in the kinetic modeling of the NO oxidation on a $Pt/Al_2O_3$ catalyst, Olsson *et al.* (63) have used 114 kJ/mol for the activation energy of desorption of NO using literature data on Pt(111). This lack in values on Pt-containing catalysts is probably because on these solids several processes such as NO dissociation and formation of other adsorbed species on the support overlap the NO adsorption/desorption processes leading to difficulties in applying classical analytical methods (TPD and calorimetry). However, by kinetic modeling of the CO/NO reaction at 573 K on $Pt/Al_2O_3$, Granger *et al.* (65) have determined the adsorption coefficient of NO ($K_{NO} = 15\ atm^{-1} = 1.5 \times 10^{-4}\ Pa^{-1}$) and CO ($K_{CO} = 127\ atm^{-1} = 1.27\,10^{-3}\ Pa^{-1}$). Considering expression [1] for the adsorption coefficient, the above values lead to heats of adsorption of 96 and 105 kJ/mol for NO and CO, respectively. Figure 9 shows that $\theta_L \approx 1$ at 573 K for the L NO species, indicating that the heat of adsorption at 573 K is ≈105 kJ/mol, which is in agreement with 96 kJ/mol obtained from the data of Ref. (65). Similarly, coverage of the L CO species at 573 K is ≈1 and its heat of adsorption is 110 kJ/mol (9–10), in agreement with 105 kJ/mol obtained from the values of Ref. (65).

## 5. CONCLUSIONS

The following conclusions are derived from the present study on the determination of the heat of adsorption of NO on a 2.9% $Pt/Al_2O_3$ catalyst.

(a) Adsorption of 1% NO/He at 300 K on the reduced solid leads to the formation of several adsorbed species on the Pt particles and on the support.

(b) IR bands are detected at 1764 and 1710 $cm^{-1}$; these are assigned to linear NO species on defect and terrace sites of the Pt particles, respectively.

(c) During the increase in the adsorption temperature, the IR band at 1710 $cm^{-1}$ disappears due to two processes: a reconstruction of the Pt surface, leading to an increase in the intensity of the IR band at 1764 $cm^{-1}$, and the strong adsorption of oxygen species.

(d) The intensities of the IR band of the linear NO species on defect sites with the adsorption temperature $T_a$, recorded under adsorption equilibrium conditions ($T_a$ varying from 300 to 680 K with $P_a = 10^3$ Pa), can be used for the determination of the evolution of the coverage $\theta_L$ of this adsorbed species as a function of $T_a$.

(e) The curve $\theta_L = f(T_a)$ leads to the determination of the heats of adsorption of the L NO species on defect sites using an adsorption model.

(f) The heat of adsorption of the L NO species linearly varies with its coverage from $E_0 = 135$ kJ/mol at $\theta_L = 0$ to $E_1 = 105$ kJ/mol at $\theta_L = 1$. The NO dissociation at high temperature does not disturb the measurements.

The above values are in agreement with those obtained by other analytical methods on single crystals and polycrystalline Pt solids (foil and filament). This shows that the analytical procedure previously developed to determine the heat of adsorption of linear and bridged CO species on several supported metal catalysts (8–16) can also be applied to NO species. To our knowledge it is the first time that the heat of adsorption of NO on a supported Pt catalyst has been determined by a direct method.

## ACKNOWLEDGMENTS

We acknowledge with pleasure the FAURECIA Industries (Bavans, France) for its financial support and the M.E.R.T (Ministère de l'Education Nationale, de la Recherche et de la Technologie) for the research fellowship to A.B.

## REFERENCES

1. Boudart, M., *in* "Handbook of Heterogeneous Catalysis" (G. Ert, H. Knözinger, and J. Weitkamps, Eds.), Vol. 1, p. 1. Wiley, New York, 1997.
2. Sachtler, W. M. H., *in* "Handbook of Heterogeneous Catalysis" (G. Ert, H. Knözinger, and J. Weitkamps, Eds.), Vol. 3, p. 1077. Wiley, New York, (1997).
3. Demmin, R. A., and Gorte, R. J., *J. Catal.* **90**, 32 (1984).
4. Herz, R. K., Kiela, J. B., and Marin, S. P., *J. Catal.* **73**, 66 (1982).
5. Sen, B., and Vannice, M. A., *J. Catal.* **130**, 9 (1991).
6. Sharma, S. B., Miller, J. T., and Dumesic, J. A., *J. Catal.* **148**, 198 (1994).
7. Tompkins, F. C., "Chemisorption of Gases on Metal." Academic Press, London, 1978.
8. Chafik, T., Dulaurent, O., Gass, J. L., and Bianchi, D., *J. Catal.* **179**, 503 (1998).

9. Dulaurent, O., and Bianchi, D., *Appl. Catal. A*. **196**, 271 (2000).
10. Bourane, A, Dulaurent, O., and D. Bianchi, D., *J. Catal.* **196**, 115 (2000).
11. Dulaurent, O., Chandes, K., Bouly, C., and Bianchi, D., *J. Catal.* **188**, 237 (1999).
12. Dulaurent, O., Chandes, K., Bouly, C., and Bianchi, D., *J. Catal.* **192**, 262 (2000).
13. Dulaurent, O., Nawdali, M., Bourane, A., and Bianchi, D., *Appl. Catal. A*. **201**, 271 (2000).
14. Dulaurent, O., Courtois, X., Perrichon, V., and Bianchi, D., *J. Phys. Chem*. **104**, 6001 (2000).
15. Dulaurent, O., Chandes, K., Bouly, C., and Bianchi, D., *J. Catal.* **192**, 273 (2000).
16. Dulaurent, O., and Bianchi, D., *Appl. Catal. A* **207**, 211 (2001).
17. Bourane, A., Dulaurent, O., and D. Bianchi, D., *J. Catal.* **195**, 406 (2000).
18. Regalbuto, J. R., and Wolf, E. E., *J. Catal.* **109**, 12 (1988).
19. Lim, K. J., Löffler, D. G., and Boudart, M., *J. Catal.* **100**, 158 (1986).
20. Lévy, P. J., Pitchon, V., Perrichon, V., Primet, M., Chevrier, M., and Gauthier, C., *J. Catal.* **178**, 363 (1998).
21. Keiski, R. L., Harkonen, M., Lahti, A., Maunula, T., Savimaki, A., and Slotte, T., *Stud. Surf. Sci. Catal.* **96**, 85 (1995).
22. Gland, J. L., and Sexton, B. A., *Surf. Sci.* **94**, 355 (1980).
23. Hayden, B. E., *Surf. Sci.* **131**, 419 (1983).
24. Heiz, U., Xu, J., and Yates, J. T., Jr., *J. Chem. Phys.* **100**, 3925 (1994).
25. Solymosi, F., and Rasko, J., *J. Catal.* **62**, 253 (1980).
26. Amirnazmi, A., and Boudart, M., *J. Catal.* **39**, 383 (1975).
27. Amirnazmi, A., Benson, J. E., and Boudart, M., *J. Catal.* **30**, 55 (1973).
28. Gardner, P., Tushaus, M., Martin, R., and Bradshaw, A. M., *Surf. Sci.* **240**, 112 (1990).
29. Pirug, G., Bonzel, H. P., Hopster, H., and Ibach, H., *J. Chem. Phys.* **71**, 593 (1979).
30. Gorte, R. J., and Gland, J. L., *Surf. Sci.* **102**, 348 (1981).
31. Levoguer, C. L., and Nix, R. M., *Surf. Sci.* **365**, 672 (1996).
32. Agrawal, V. K., and Trenary, M., *Surf. Sci.* **259**, 116 (1991).
33. Van Slooten, R. F., and Nieuwenhuys, B. E., *J. Catal.* **122**, 429 (1990).
34. Fang, S. M., and White, J. M., *J. Catal.* **83**, 1 (1983).
35. Brown, M. F., and Gonzalez, R. D., *J. Catal.* **44**, 477 (1976).
36. Westerberg, B., and Fridell, E., *J. Mol. Catal. A* **165**, 249 (2001).
37. Underwood, G. M., Miller, T. M., and Grassian, V. H., *J. Phys. Chem.* **103**, 6184 (1999).
38. Nakamoto, K., "Infrared Spectra of Inorganic and Coordination Compounds." Wiley, New York, 1970.
39. Goodman, A. L., Miller, T. M., and. Grassian, V. H., *J. Vac Sci. Technol. A*. **16**, 2585 (1998).
40. Kijlstra, W. S., Brands, D. S., Poels, E. K., and Bliek, A., *J. Catal.* **171**, 208 (1997).
41. Glasstone, S., Laidler, K. J., and Eyring, H., *in* "The Theory of Rate Processes." McGraw-Hill, New York, 1941.
42. Laidler, K. J., *Catalysis* **1**, 75 (1954).
43. Bourane, A., and Bianchi, D., *J. Catal.* **202**, 34 (2001).
44. Bourane, A., Dulaurent, O., and D. Bianchi, D., *Langmuir* **17**, 5496 (2001).
45. Bourane, A., Dulaurent, O., Chandes, K., and Bianchi, D., *Appl. Catal. A* **214**, 193 (2001).
46. Lambert, R. M., and Comrie, C. M., *Surf. Sci.* **46**, 61 (1974).
47. Gland, J. L., *Surf. Sci.* **71**, 327 (1978).
48. Lin, T. H., and Somorjai, G. A., *Surf. Sci.* **107**, 573 (1981).
49. Gorte, R. J., Schmidt, L. D., and Gland, J. L., *Surf. Sci.* **109**, 367 (1981).
50. Serri, J. A., Tully, J. C., and Cardillo, M. J., *J. Chem Phys.* **79**, 1530 (1983).
51. Banholzer, W. F., and Masel, R. I., *J. Catal.* **85**, 127 (1984).
52. Gohndrone, J. M. and Masel, R. I., *Surf. Sci.* **209**, 44 (1989).
53. Wickham, D. T., Banse, B. A., and Koel, B. E., *Surf. Sci.* **223**, 82 (1989).
54. Campbell, C. T., Ertl, G., and Segner, J., *Surf. Sci.* **115**, 309 (1982).
55. Miki, H., Nagase, T., Kioka, T., Sugai, S., and Kawasaki, K., *Surf. Sci.* **225**, 1 (1990).
56. Zafiris, G. S., and Gorte, R. J., *Surf. Sci.* **276**, 86 (1992).
57. Altmann, E. I., and Gorte, R. J., *J. Phys. Chem*. **93**, 1993 (1989).
58. Xu, J., and Yates, J. T., Jr., *Surf. Sci.* **327**, 193 (1995).
59. Xu, J., Henriksen, P. N., and Yates, J. T. Jr., *Langmuir* **10**, 3663 (1994).
60. Lee, W. T., Ford, L., Blowers, P., Nigg, H. L., and Masel, R. I., *Surf. Sci.* **416**, 141 (1998).
61. Yeo, Y. Y., Vattuone, L., and King, D. A., *J. Chem. Phys.* **104**, 3810 (1996).
62. Fukutani, K., Magkoev, T. T., Murata, Y., and Terakura, K., *Surf. Sci.* **363**, 185 (1996).
63. Olsson, L., Westerberg, B., Persson, H., Fridell, E., Skoglundh M., and Andersson, B., *J. Phys. Chem. B* **103**, 10433 (1999).
64. Wartnaby, C. E., Stuck, A., Yeo, Y. Y., and King, D. A., *J. Chem Phys.* **102**, 1855 (1995).
65. Granger, P., Dathy, C., Lecomte, J. J., Leclercq, L., Prigent, M., Mabilon, G., and Leclercq, G., *J. Catal.* **173**, 304 (1998).